Supplemental file

An In Vitro Quantitative Systems Pharmacology Platform for Characterizing CD3-Bispecific Antibody-Mediated T-Cell Activation and Tumor Cell Cytotoxicity

Xuanzhen Yuan[a], Craig Thalhauser[b], Nasrin Afzal[b], Kristel Kemper[b], Guohua An[a,*], Tommy Li[b,*]

[a]Department of Pharmaceutical Sciences and Experimental Therapeutics, College of Pharmacy, University of Iowa, Iowa City, Iowa, USA

[b]Genmab, Princeton, New Jersey, USA

[*]Correspondence:

Tommy Li (toli@genmab.com)

Guohua An (guohua-an@uiowa.edu)

Table S1. **List of solid tumor cell lines and their corresponding absolute expression level of 5T4 proteins**

	Tumor cell line	Indication	5T4 expression (molecule/cell)
1	SiHa	Cervical cancer	9,447
2	BxPC-3	Pancreatic cancer	12,398
3	MDA-MB-231	Breast cancer	13,524
4	PANC-1	Pancreatic cancer	16,500
5	FaDu	Head and neck cancer	17,925
6	EPLC-272H	Lung cancer	20,106
7	SW780	Bladder cancer	21,775
8	Ca Ski	Cervical cancer	22,629
9	RT-112	Bladder cancer	23,917
10	MDA-MB-468	Breast cancer	31,582
11	PC-3	Prostate cancer	35,800
12	SCC-9	Head and neck cancer	36,102
13	SK-GT-4	Esophageal cancer	55,545
14	DU 145	Prostate cancer	61,686

Table S2. **Overview of in vitro data for T-cell activation and tumor cell cytotoxicity**

	Number of unique assay conditions	Number of total observations	E:T ratio	CD3 binding affinity (nM)	5T4 binding affinity (nM)	T-cell donors	Time points (hr)
T-cell activation data							
MDA-MB-231	8	24	4:1	683	3	NA	24, 48, 72
MDA-MB-468	8	24	4:1	683	3	NA	24, 48, 72
Tumor cell cytotoxicity data							
MDA-MB-231	51	202	4:1	683	3	5 donors & NA	24, 48, 72
	9	9	8:1	16	3	NA	72
MDA-MB-468	98	312	4:1	683	3	10 donors & NA	24, 48, 72
	16	16	1:1, 2:1	683	3	NA	72
	17	17	8:1	16, 683	3	NA	72
12 other solid tumor cell lines	486	969	4:1	683	3	23 donors	72

Note: each unique assay condition is defined by a distinct combination of tumor cell line, drug concentration, E:T ratio, CD3 binding affinity, and T-cell donor.
NA: T-cell donor was not available for this study

Table S3. **Tumor cell line covariate clusters for EC50_act and Max_kill**

Covariate cluster group	Tumor cell line	Note
	EC50_act	
Group 1	SCC-9, SW780, BxPC-3, Ca Ski, DU 145, EPLC272H, RT-112, SiHa, FaDu, PANC-1, PC-3, SK-GT-4	No activation data
Group 2	MDA-MB-231	Activation data available
Group 3	MDA-MB-468	Activation data available
	Max_kill	
Group 1	SCC-9, SW780	High killing resistance
Group 2	BxPC-3, Ca Ski	Relatively high killing resistance
Group 3	DU 145, EPLC272H, MDA-MB-231, RT-112, SiHa	Relatively low killing resistance
Group 4	FaDu, MDA-MB-468, PANC-1, PC-3, SK-GT-4	Low killing resistance

Table S4. **T-cell donor covariate clusters for Max_kill**

Covariate cluster group for Max_kill	T-cell donor
Group 1	7, 14, 24, 29
Group 2	1, 3, 5, 6, 8, 9, 10, 11, 12, 13, 15, 16, 17, 18, 20, 21, 22, 23, 25, 26, 27, 30, NA
Group 3	2, 4, 19, 28

NA indicates donor source was not available for this study

Table S5. Model-estimated trimer threshold (EC50_act) and maximal killing rate constant (Max_kill), stratified by tumor cell line and T-cell donor

Parameter	Unit	Definition	Estimate	RSE%
$EC50\_act_{(Cell\_Line\_group1)}$	trimers/T cell	Trimer EC50 for T-cell activation	3.69	7.8
$EC50\_act_{(Cell\_Line\_group2)}$			4.60	7.7
$EC50\_act_{(Cell\_Line\_group3)}$			2.13	8.5
$Max\_kill_{(Cell\_Line\_group1,\ Donor\_group1)}$	$hr^{-1} \times$ effector T $cell^{-1}$	Maximum rate constant for tumor cell killing	9.13E-06	26.2
$Max\_kill_{(Cell\_Line\_group1,\ Donor\_group2)}$			9.35E-07	15.0
$Max\_kill_{(Cell\_Line\_group1,\ Donor\_group3)}$			6.39E-07	17.1
$Max\_kill_{(Cell\_Line\_group2,\ Donor\_group1)}$			2.41E-05	27.6
$Max\_kill_{(Cell\_Line\_group2,\ Donor\_group2)}$			2.46E-06	17.0
$Max\_kill_{(Cell\_Line\_group2,\ Donor\_group3)}$			1.69E-06	18.9
$Max\_kill_{(Cell\_Line\_group3,\ Donor\_group1)}$			4.15E-05	22.7
$Max\_kill_{(Cell\_Line\_group3,\ Donor\_group2)}$			4.24E-06	8.4
$Max\_kill_{(Cell\_Line\_group3,\ Donor\_group3)}$			2.90E-06	11.6
$Max\_kill_{(Cell\_Line\_group4,\ Donor\_group1)}$			1.27E-04	24.5
$Max\_kill_{(Cell\_Line\_group4,\ Donor\_group2)}$			1.30E-05	12.0
$Max\_kill_{(Cell\_Line\_group4,\ Donor\_group3)}$			8.88E-06	14.5

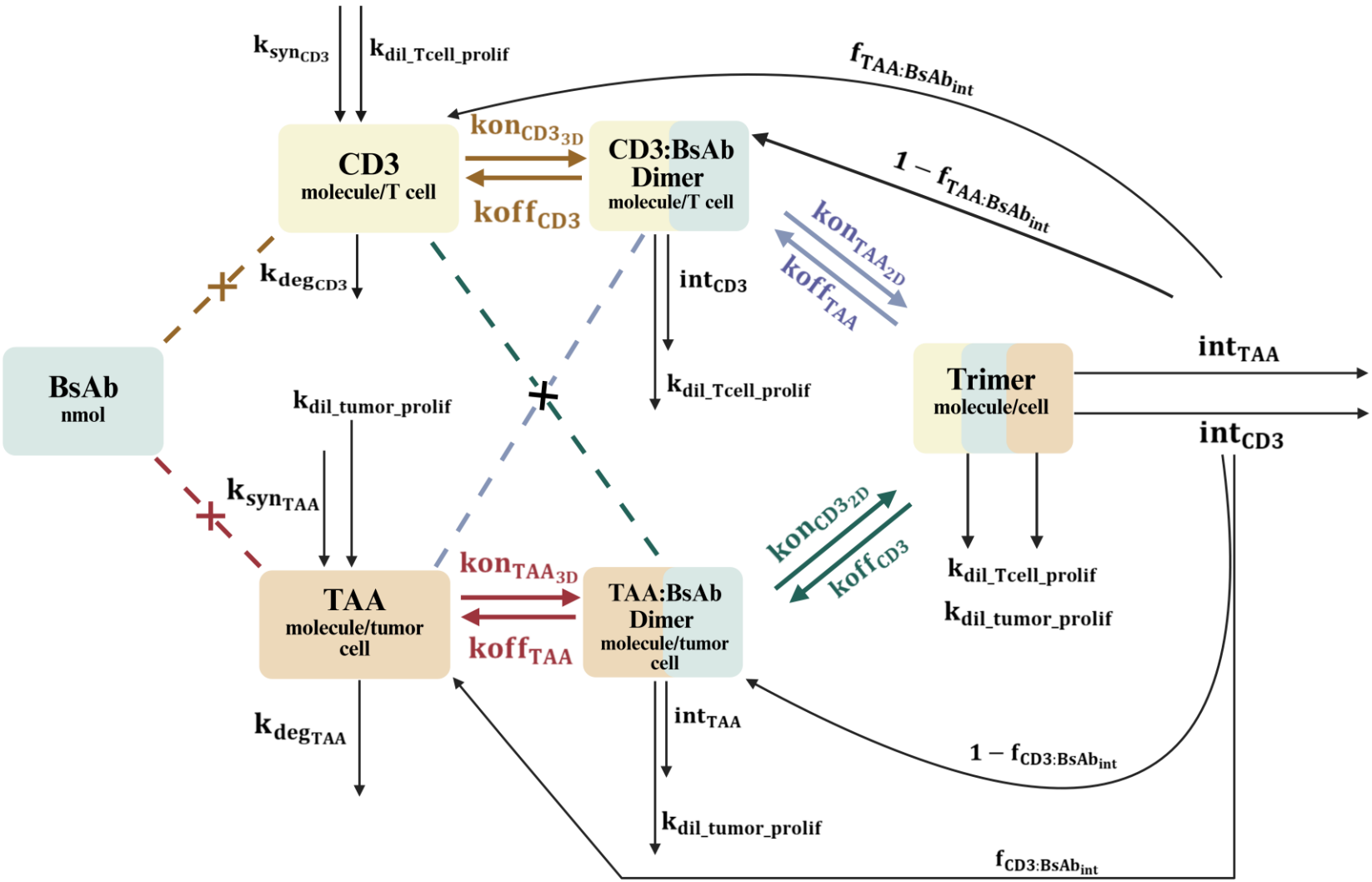
$k_{syn_{CD3}}$
$k_{dil\_Tcell\_prolif}$
$f_{TAA:BsAb_{int}}$
CD3
molecule/T cell
$kon_{CD3_{3D}}$
$koff_{CD3}$
CD3:BsAb Dimer
molecule/T cell
$1 - f_{TAA:BsAb_{int}}$
$kon_{TAA_{2D}}$
$koff_{TAA}$
$k_{deg_{CD3}}$
int_{CD3}
$k_{dil\_Tcell\_prolif}$
BsAb
nmol
$k_{dil\_tumor\_prolif}$
Trimer
molecule/cell
int_{TAA}
int_{CD3}
$k_{syn_{TAA}}$
$kon_{CD3_{2D}}$
$koff_{CD3}$
$k_{dil\_Tcell\_prolif}$
$k_{dil\_tumor\_prolif}$
$kon_{TAA_{3D}}$
TAA
molecule/tumor cell
$koff_{TAA}$
TAA:BsAb Dimer
molecule/tumor cell
$k_{deg_{TAA}}$
int_{TAA}
$1 - f_{CD3:BsAb_{int}}$
$k_{dil\_tumor\_prolif}$
$f_{CD3:BsAb_{int}}$

Fig. S1 The structure of base trimer formation sub-model (E:T ratio=1:1 scenario)

This per-cell model tracks the average quantity of CD3 and CD3:BsAb dimer per T cell, TAA and TAA:BsAb dimer per tumor cell, and trimer per cell. Free bispecific antibodies (BsAbs) bind CD3 or TAA to form dimers (CD3:BsAb or TAA:BsAb) via second-order association constants ($kon_{TAA_{3D}}$ or $kon_{CD3_{3D}}$). Dimers either dissociate back to free targets and BsAb with first-order dissociation rate constants ($koff_{CD3}$ or $koff_{TAA}$), or crosslink with the other free targets to form trimers via second-order association constants ($kon_{TAA_{2D}}$ or $kon_{CD3_{2D}}$). Trimers can dissociate back to free targets and dimers with the same corresponding koff values. Dimers internalize with first-order rate constants (int_{CD3} and int_{TAA}). For trimer internalization via the TAA side, a fraction ($f_{TAA:BsAb_{int}}$) of the trimers split to free CD3 and TAA:BsAb and the remaining fraction of the trimers split to free TAA and CD3:BsAb. CD3-associated species will be recycled back to their respective compartments. CD3-side internalization is symmetric, with TAA-associated species recycling to the TAA-relevant compartments. Free CD3/TAA targets undergo synthesis and natural degradation via first-order synthesis rate constants (k_{synCD3} or k_{synTAA}) and degradation rate constants (k_{degCD3} or k_{degTAA}). The proliferation of T cells and tumor cells increases free-target abundance and dilutes dimer/trimer density on the representative single T cell and tumor cell at first-order rate constants $k_{dil\_Tcell\_prolif}$ and $k_{dil\_tumor\_prolif}$. The figure was created with BioRender.com.

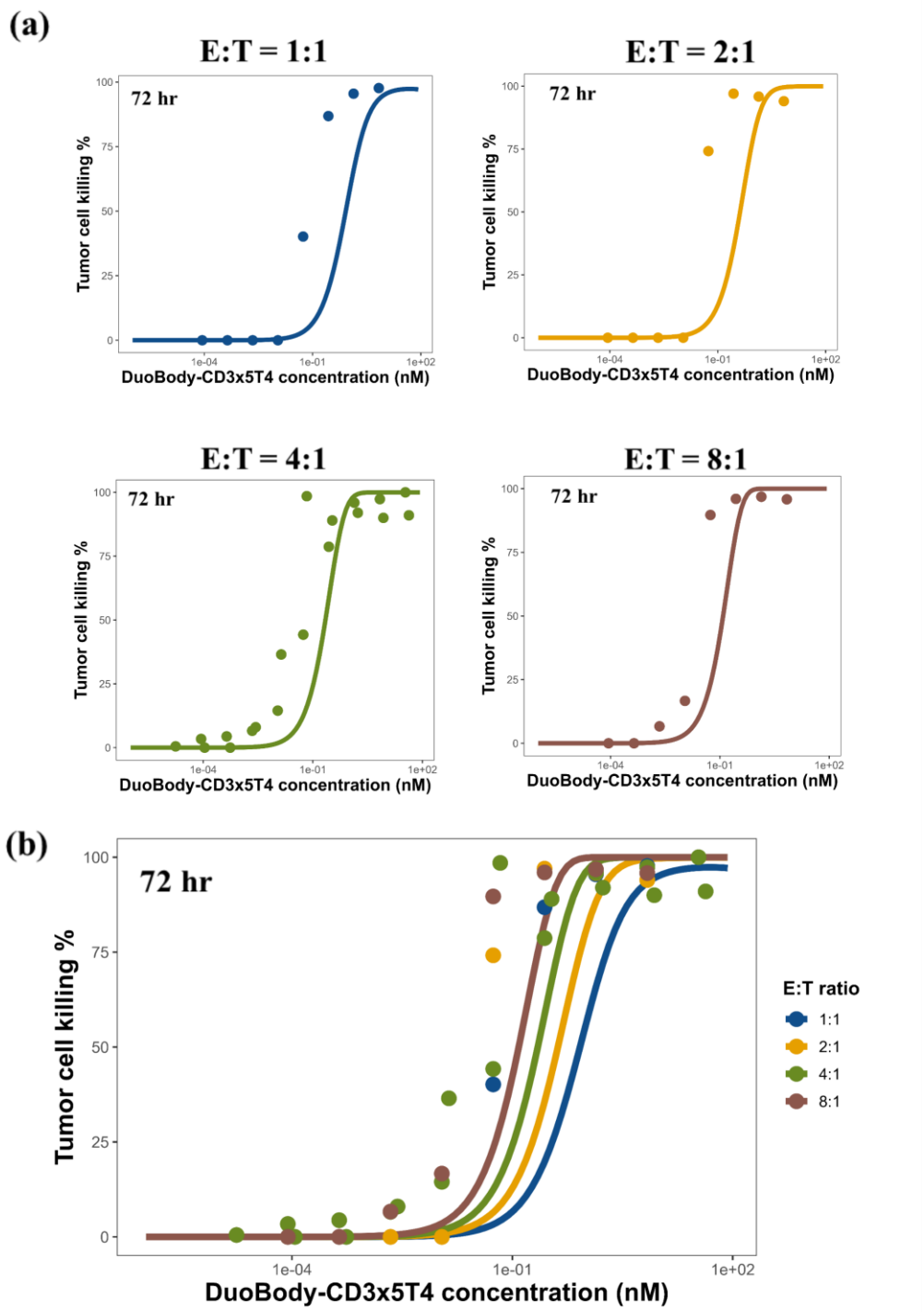

Fig. S2 Effector-to-target (E:T) ratios on DuoBody-CD3x5T4-mediated tumor cell killing at 72 hr in the MDA-MB-468 cell line, estimated by the base QSP model incorporating the base trimer formation sub-model and the base tumor killing sub-model. (a) Cytotoxicity-concentration profiles, shown separately for E:T ratio = 1:1, 2:1, 4:1, and 8:1. (b) Overlay of the cytotoxicity-concentration profiles across four E:T ratios. Symbols represent means of observed data and solid lines represent model estimations.

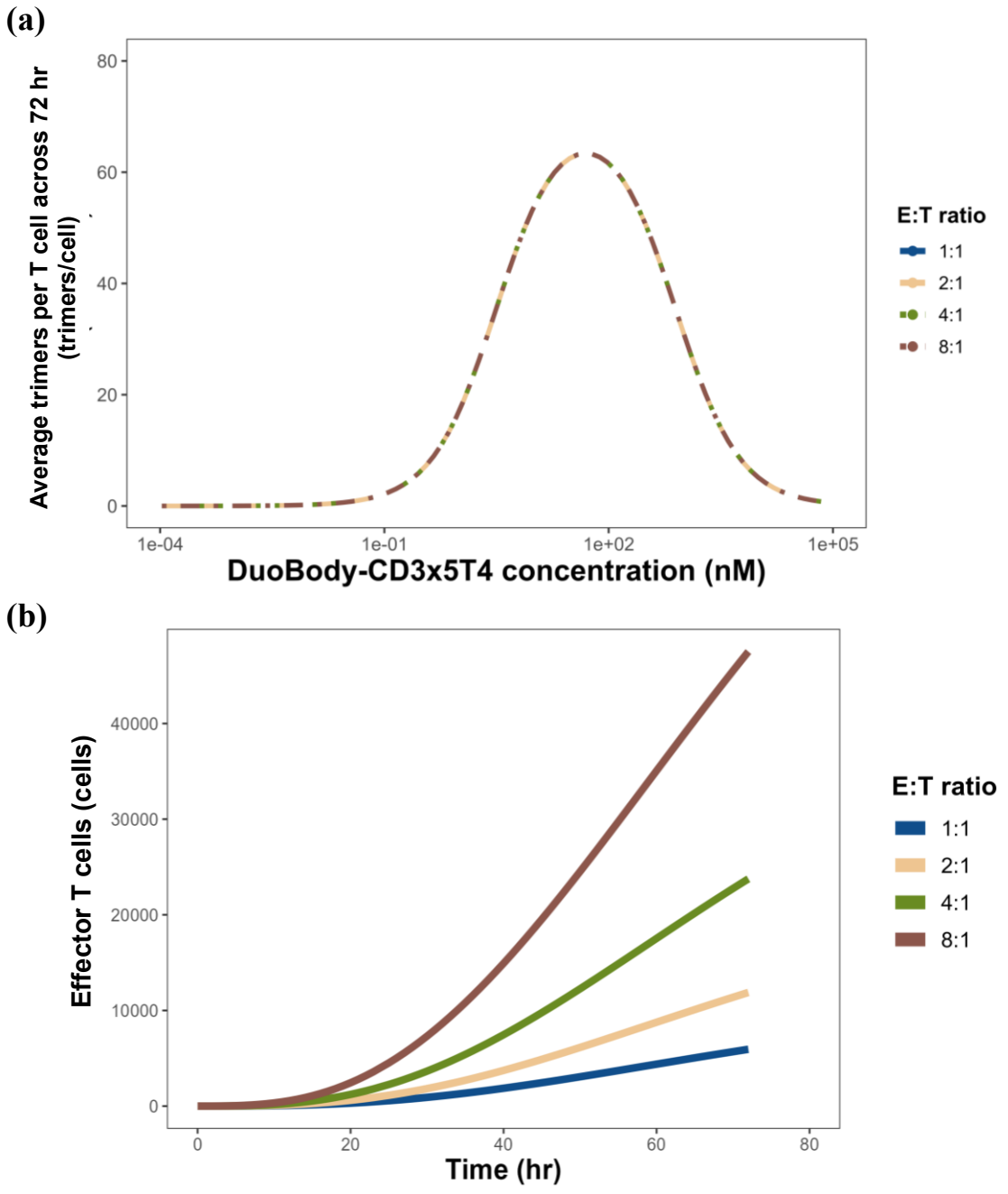

Fig. S3 Impact of effector-to-target (E:T) ratios on DuoBody-CD3x5T4-mediated trimer formation and effector T-cell numbers in MDA-MB-468 cell line, predicted by the base QSP model incorporating the base trimer formation sub-model and base tumor killing sub-model. (a) Predicted time-averaged trimers per T cell (0-72 hr) versus drug concentration across four E:T ratios. (b) Predicted effector T cell-concentration profiles across four E:T ratios, following 6.86 nM DuoBody-CD3x5T4.

Poor fit of the base QSP model and underlying causes

Fig. S2 presents calibrated tumor cell cytotoxicity-concentration profiles across four E:T ratios, generated with the base QSP model (without R_{ET}) incorporating the base trimer formation sub-model (**Fig. S1**). In that case, the cytotoxicity-concentration curves were right-shifted relative to the observed data, with larger shift at lower E:T ratios. Simulations based on the base QSP model (**Fig. S3**) clarify the cause: without $R_{ET,}$ the model yielded identical trimers per T cell across E:T ratios while producing more effector T cells at higher E:T ratios due to larger initial T-cell inputs. This combination inflated apparent potency differences across E:T ratios (i.e., lower E:T ratios predicted lower cytotoxicity potency) and failed to match observed data.

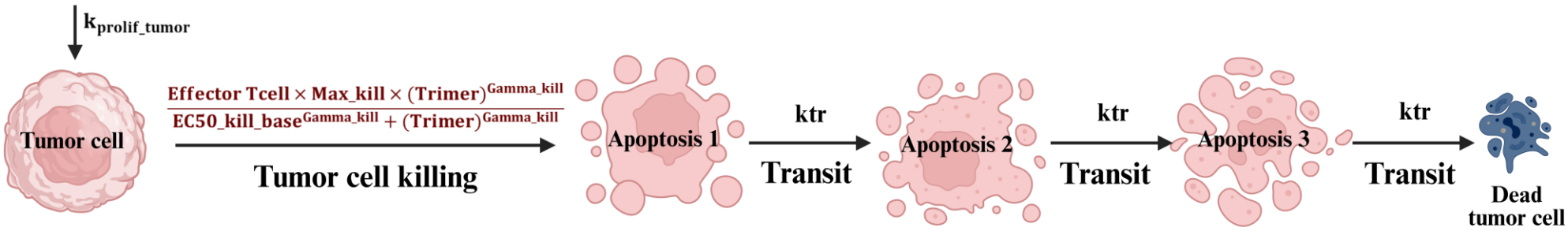

Fig. S4 The structure of base tumor cell killing sub-model. Tumor cells proliferate at rate constant: k_{prolif_tumor}. The per-effector rate of tumor cell killing follows Hill function, primarily driven by average number of trimers on the representative T cell, parameterized with maximal per-effector killing rate constant (Max_kill), the trimer density required to achieve half-maximal per-effector killing rate constant (EC50_kill_base), and the Hill coefficient (Gamma_kill). Once targeted, tumor cells pass through three apoptosis transit stages with transit rate constant (ktr) to death. The figure was created with BioRender.com.

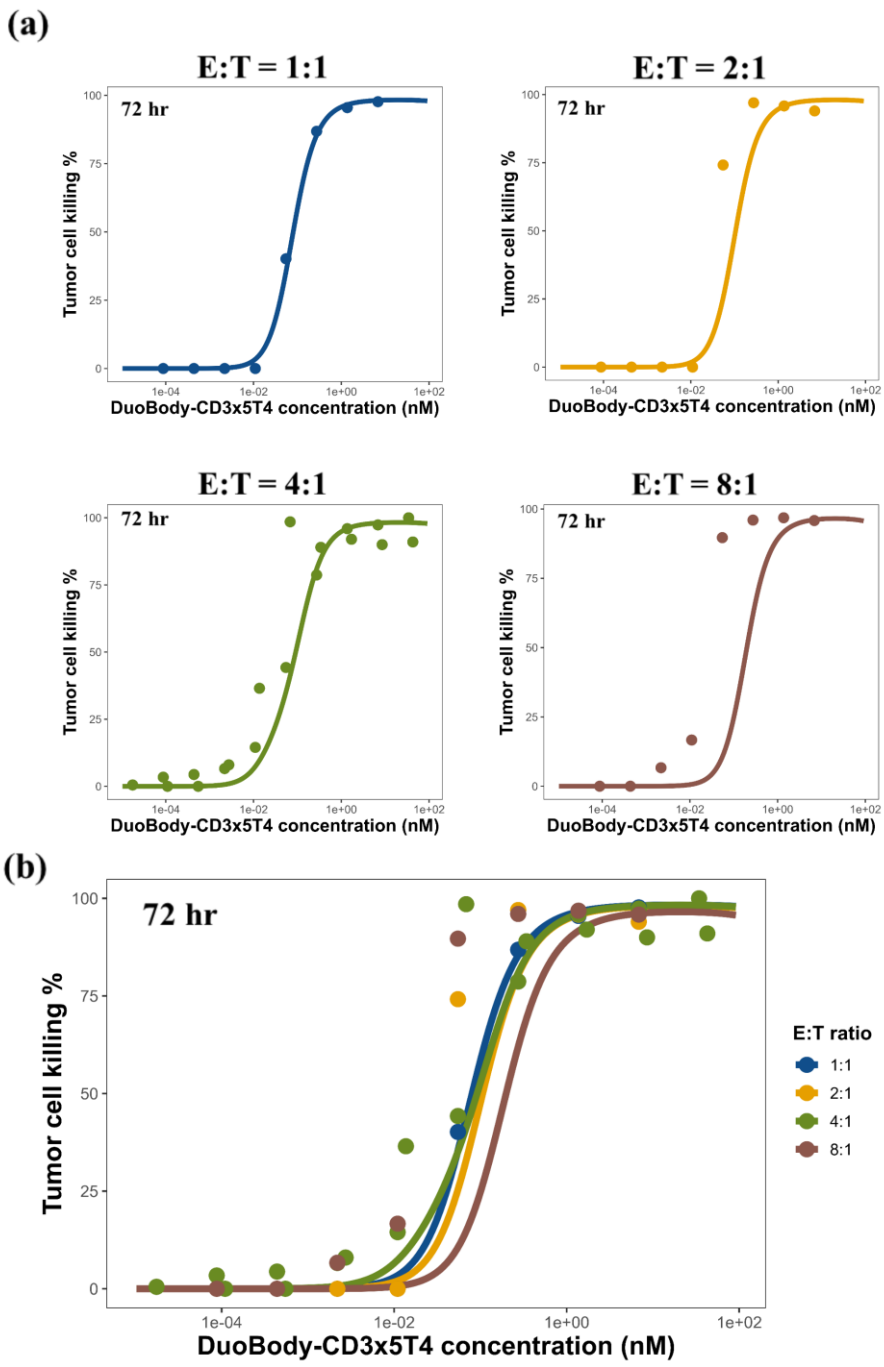

Fig. S5 Effector-to-target (E:T) ratios on DuoBody-CD3x5T4-mediated tumor cell killing at 72 hr in the MDA-MB-468 cell line, estimated by the intermediate QSP model incorporating the final trimer formation sub-model and base tumor cell killing sub-model (Eq. S16). (a) Cytotoxicity-concentration profiles, shown separately for E:T ratio = 1:1, 2:1, 4:1, and 8:1. (b) Overlay of the cytotoxicity-concentration profiles across four E:T ratios. Symbols represent means of observed data and solid lines represent model estimations.

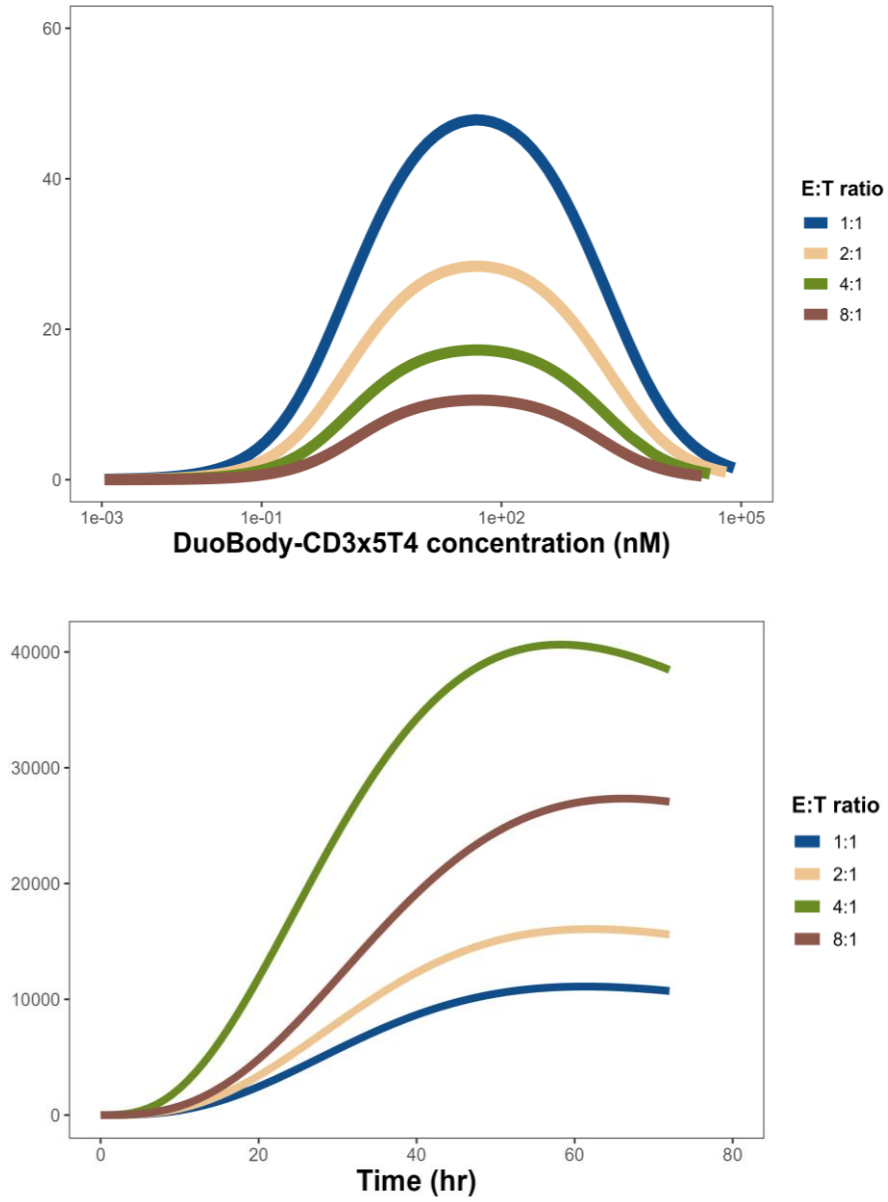

Fig. S6 Impact of effector-to-target (E:T) ratios on DuoBody-CD3x5T4-mediated trimer formation and effector T-cell numbers in MDA-MB-468 cell line, predicted by the intermediate QSP model incorporating the final trimer formation sub-model and base tumor cell killing equation (Eq. S16). (a) Predicted time-averaged trimer per T cell (0-72 hr) versus drug concentration across four E:T ratios. (b) Predicted effector T cell-concentration profiles across four E:T ratios, following 6.86 nM DuoBody-CD3x5T4.

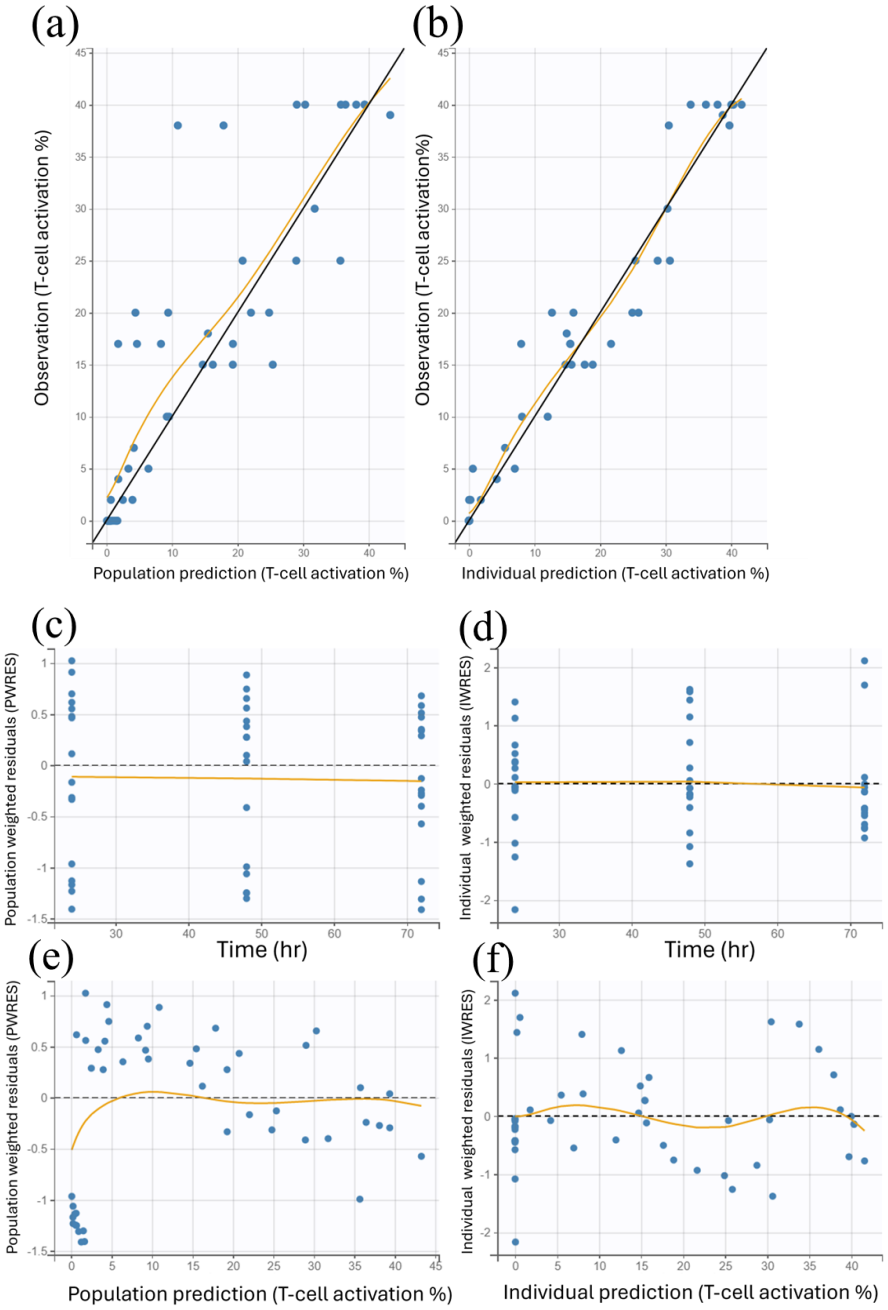

Fig. S7 Goodness-of-fit plots for T-cell activation. (a) Observed T-cell activation vs. population predicted T-cell activation. (b) Observed T-cell activation vs. individual predicted T-cell activation. (c) Population weighted residuals vs. time. (d) Individual weighted residuals vs. time. (e) Population weighted residuals vs. population predicted T-cell activation. (f) Individual weighted residuals vs. individual predicted T-cell activation. Dotted black lines represent either the line of identity or zero line. Yellow lines represent the spline interpolation.

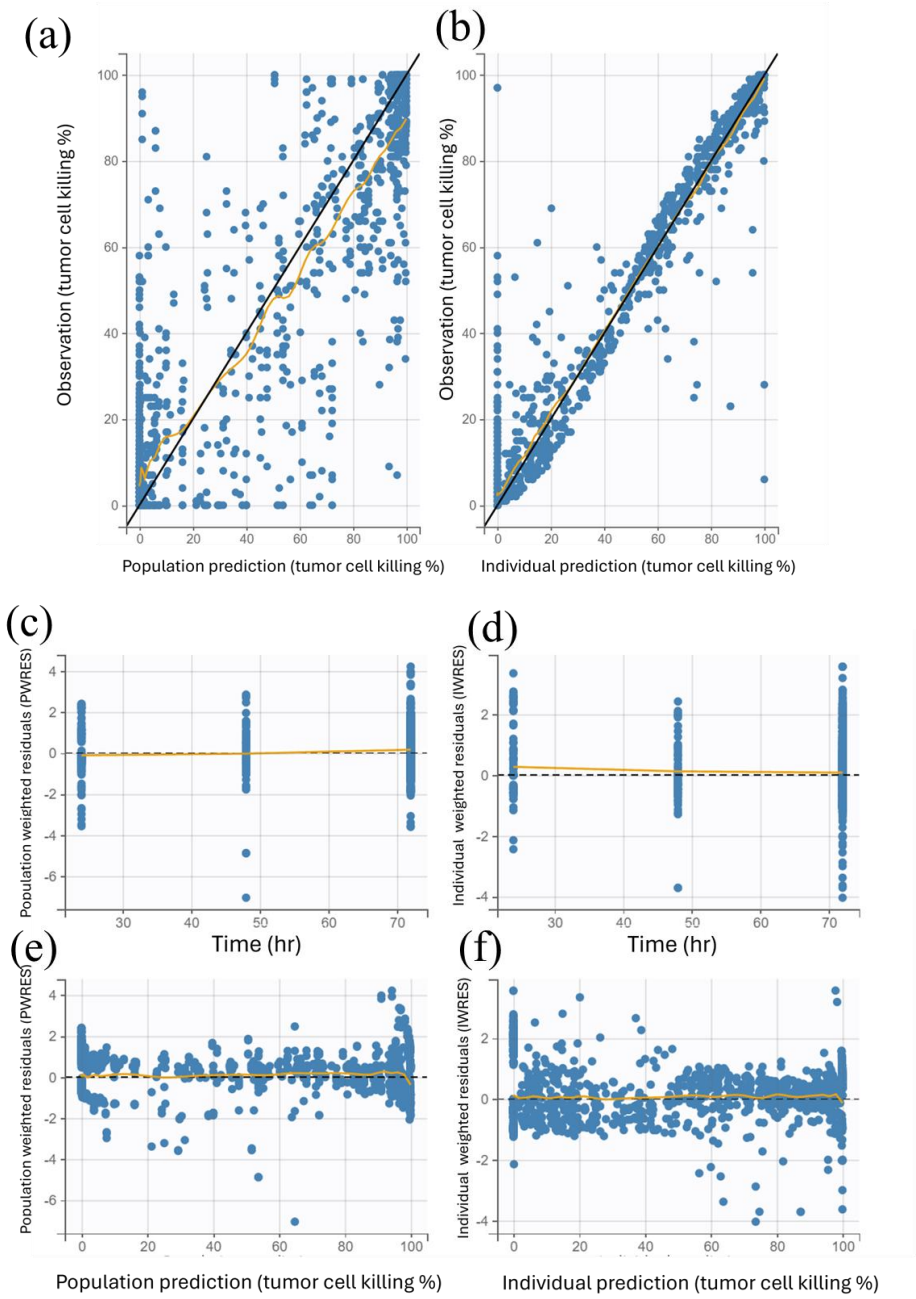

Fig. S8 Goodness-of-fit plots for tumor cell killing. (a) Observed tumor cell killing vs. population predicted tumor cell killing. (b) Observed tumor cell killing vs. individual predicted tumor cell killing. (c) Population weighted residuals vs. time. (d) Individual weighted residuals vs. time. (e) Population weighted residuals vs. population predicted tumor cell killing. (f) Individual weighted residuals vs. individual predicted tumor cell killing. Dotted black lines represent either the line of identity or zero line. Yellow lines represent the spline interpolation.

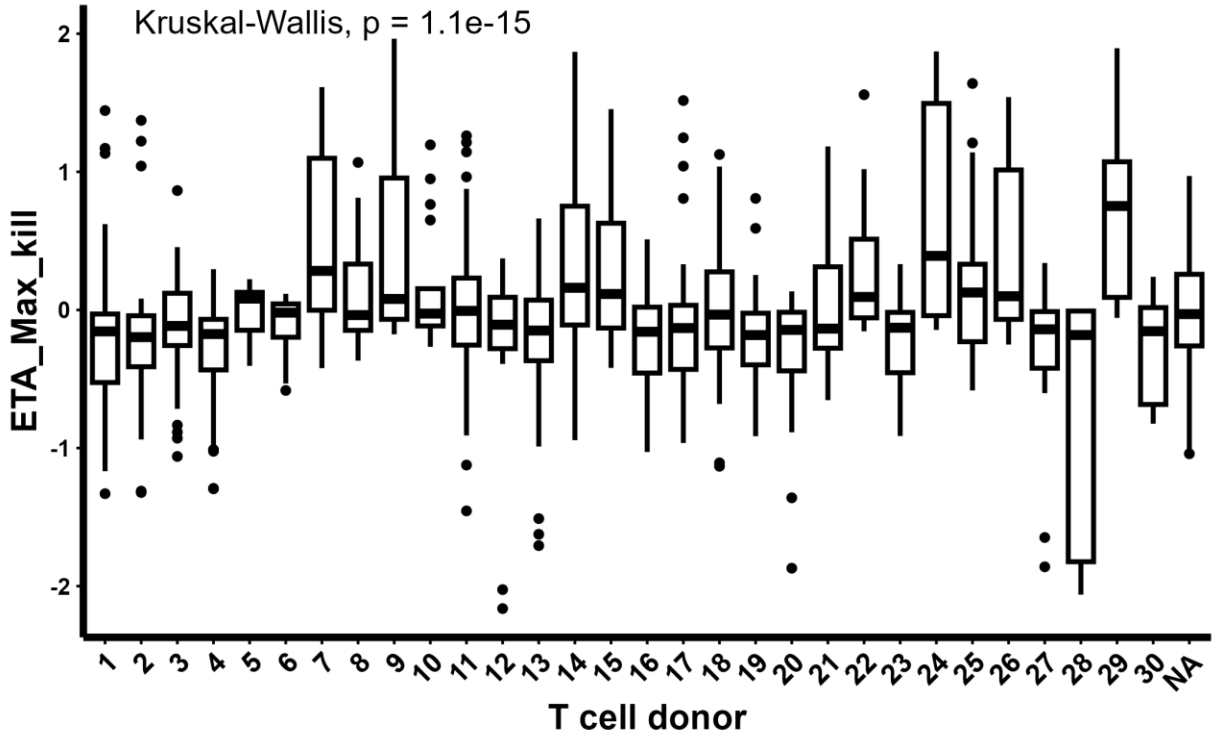

Fig. S9 Distribution of random effects (ETA) for parameter Max_kill across T-cell donors. The individual estimates of the ETA were obtained from the base model without covariates.

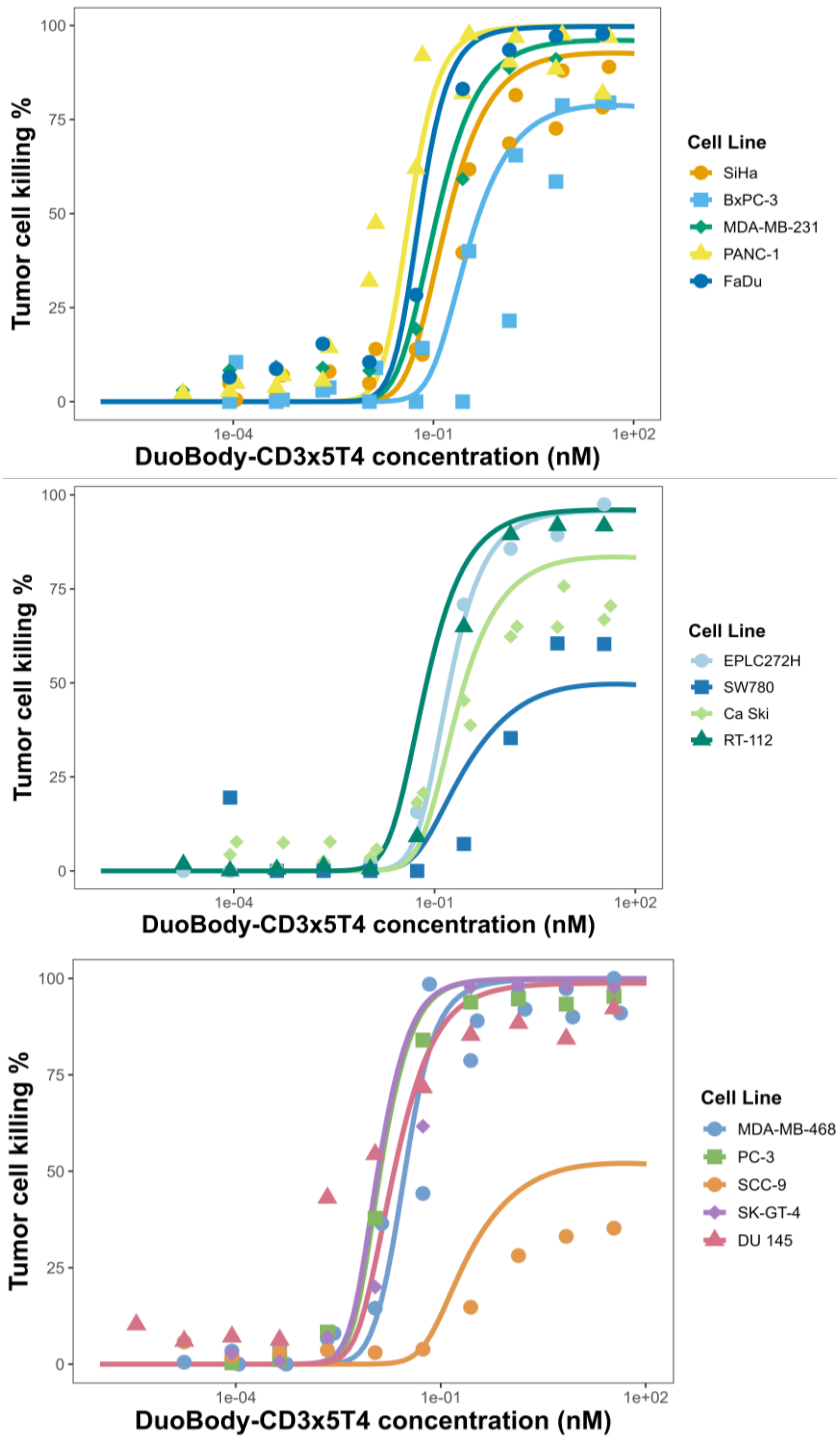

Fig. S10 Tumor cell cytotoxicity-DuoBody-CD3x5T4 concentration profiles at 72 hr, grouped by 5T4 expression ranges. (a) low 5T4 expression range (9,447−17,925 molecule/cell); (b) medium 5T4 expression range (20,106−23,917 molecule/cell); (c) high 5T4 expression range (31,582−61,686 molecule/cell). All groups were generated under an effector-to-target (E:T) ratio of 4:1. Symbols represent means of observed data and solid lines represent model predictions.

Equations used for parameter calculation:

$$f_{Tcell} = \frac{area_{synapse}}{sureface\ area_{Tcell}} \quad (S1)$$

$$f_{tumor} = \frac{area_{synapse}}{surface\ area_{tumor}} \quad (S2)$$

$$k_{syn_{CD3}} = k_{deg_{TAA}} \times base_{CD3} \quad (S3)$$

$$k_{syn_{TAA}} = k_{deg_{CD3}} \times base_{TAA} \quad (S4)$$

$$f_{CD3:BsAb_{int}} = \frac{koff_{TAA}}{koff_{CD3} + koff_{TAA}} \quad (S5)$$

$$f_{TAA:BsAb_{int}} = 1 - \frac{koff_{TAA}}{koff_{CD3} + koff_{TAA}} \quad (S6)$$

$$R_{ET} = \frac{Tcell_{tot}}{tumor_{tot}} \quad (S7)$$

$$Tcell_{tot} = Tr + Ta + Te \quad (S8)$$

$$k_{prolif\_Ta} = \frac{0.693}{DT_{Ta}} \quad (S9)$$

$$k_{prolif\_tumor} = \frac{0.693}{DT_{tumor}} \quad (S10)$$

$$k_{dil\_Tcell\_prolif} = \frac{k_{prolif\_Ta} \times Ta}{Tcell_{tot}} \quad (S11)$$

$$k_{dil\_tumor\_prolif} = \frac{k_{prolif\_tumor} \times tumor\_cell}{tumor_{tot}} \quad (S12)$$

$$k_{deg\_Tr} = \frac{0.693}{HL_{Tr}} \quad (S13)$$

$$k_{deg\_Ta} = \frac{0.693}{HL_{Ta}} \tag{S14}$$

$$k_{deg\_Te} = \frac{0.693}{HL_{Te}} \tag{S15}$$

Intermediate ordinary differential equations (ODEs) for tumor cells and apoptosis$_1$cells:

$$\frac{dtumor\_cell}{dt} = k_{prolif\_tumor} \times tumor_{cell} - \frac{Max\_kill \times (trimer)^{Gamma\_kill}}{EC50\_kill\_base^{Gamma\_kill} + (trimer)^{Gamma\_kill}} \times Te \times tumor\_cell \tag{S16}$$

$$tumor\_cell\,(0) = \text{initial tumor cell count}$$

$$\frac{dapoT1}{dt} = \frac{Max\_kill \times (trimer)^{Gamma\_kill}}{EC50\_kill\_base^{Gamma\_kill} + (trimer)^{Gamma\_kill}} \times Te \times tumor\_cell - ktr \times apot1$$

$$apoT1(0) = 0$$

Note: In **Eq. S16**, trimer denotes the number of trimers per T cell.